





Investigation into the writing dynamics of planar Bragg gratings using pulsed 213 nm radiation

Q. SALMAN AHMED,^{*} JAMES W. FIELD, CHRISTOPHER HOLMES,  SWE ZIN OO, PAOLO L. MENNEA, REX H. S. BANNERMAN,  ROD CECIL, GLENN CHURCHILL, CORIN B. E. GAWITH, PETER G. R. SMITH,  PAUL C. GOW,  AND JAMES C. GATES

Optoelectronics Research Centre, University of Southampton, Southampton, SO17 1BJ, UK

^{*}*qazi.salman.ahmed@soton.ac.uk*

Abstract: We present the first substantive investigation into the photosensitivity response of planar-doped silica to pulsed 213 nm light. We look at the response over a broad range of fluences and average powers to identify suitable regimes for simultaneous waveguide and Bragg grating writing. Unlike previously reported work, we do not observe any clear evidence of a similar non-linear photosensitivity response in B/Ge doped silica. We discuss laser-induced damage, saturation of photosensitivity, and grating response. This paper presents writing regimes for small spot direct UV writing where the photosensitivity and grating response are optimum, thereby confirming the suitability of the fabrication approach for complex devices.

Published by Optica Publishing Group under the terms of the [Creative Commons Attribution 4.0 License](#). Further distribution of this work must maintain attribution to the author(s) and the published article's title, journal citation, and DOI.

1. Introduction

Silica based Bragg grating structures are widely used for planar optical devices such as add-drop filter components [1], grating stabilized semiconductor lasers [2] and optical sensors [3]. Bragg grating-based devices are typically fabricated by means such as: conventional lithography [4]; femtosecond writing [5]; or UV laser writing [6].

Bragg gratings in fibers are typically classified into eight different categories [7]; these are defined by glass composition (doping and whether hydrogen loaded), laser exposure, and thermal properties [7]. The underlying mechanisms of laser-induced refractive index changes are debated [8], but it is commonly accepted that defects in the material cause the change in refractive index upon UV exposure [7]. The color centre model describes the photo-induced change in refractive index according to the Kramers-Kronig relation [9]. However, upon more prolonged UV exposure, densification is believed to have a greater impact on the induced change in the refractive index [10].

Use of phase masks is a common technique to define different types of gratings into an optical fiber core upon UV exposure [11]. However, this technique relies upon a pre-existing waveguide. In contrast, the small spot direct UV writing (SSDUW) method provides a unique ability to simultaneously inscribe channel waveguides and Bragg gratings (see Fig. 1) in planar silica with minimal losses [6]. Typically SSDUW uses a 244 nm continuous-wave (CW) laser to induce changes in the refractive index of doped silica [6]. This planar writing approach is capable of fabricating low-loss channel waveguides, couplers, Bragg gratings, and polarisers within a germanium or boron-doped silica layer by translating the substrate through a focused UV beam [12].

Recently, 213 nm pulsed laser sources have been explored as an alternative to 244 nm lasers [12–14]. Compared to conventional 244 nm sources, pulsed 213 nm sources are compact in design, and robust. The first use of 213 nm laser for UV writing in fiber was reported by Gagné

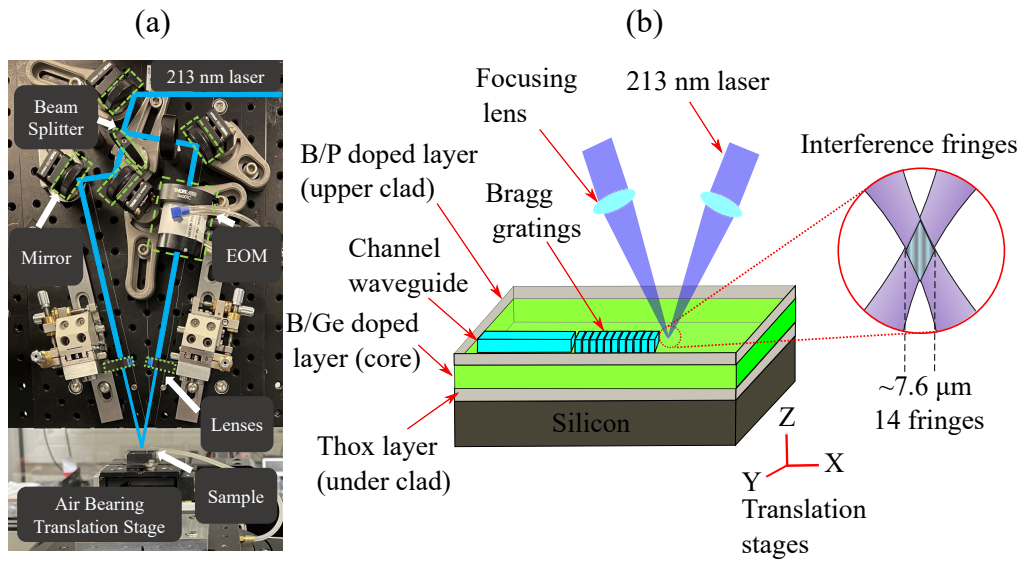


Fig. 1. (a) An annotated photograph of the 213 nm SSDUW setup. (b) Schematic of the UV writing setup; enabling inscription of waveguides and Bragg gratings simultaneously in doped silica.

and Kashyap to define strong gratings in hydrogen-free B/Ge doped fiber [11]. In their work, two-photon absorption was suggested to be a dominant mechanism for the photosensitivity of B/Ge doped fiber.

In our previous work, we have defined waveguides and high-quality Bragg gratings simultaneously in doped planar silica (hydrogen-loaded) using SSDUW with a 213 nm laser [15–17]. Fabrication of gratings in planar silica is inherently different from fiber due to the geometry, glass composition, and stresses between the layers and the silicon substrate. The typical structure we use for planar optics consists of a flame hydrolysis deposited silica core layer, doped with germanium and boron, on a silicon wafer with a 15 μm thermal oxide acting as an underclad. A thick overlaid layer doped with phosphorus and boron is usually deposited on top of the core layer (Figure S1 is available for the details of fabrication). The planar core layer does not have a predefined waveguide, using high-energy pulsed sources to define waveguide and gratings can lead to significant levels of ablation and subsurface damage to samples [16]. Therefore, it is essential to establish the optimal regimes to use these laser sources without causing damage. Prior SSDUW with constant writing power found a linear photosensitivity response to a fluence followed by saturation [16], similar to that observed for conventional 244 nm CW writing. In this work, we use a broad range of average beam powers and fluences to explore the characteristics of SSDUW, investigating the saturation of the photosensitivity response and grating properties to find the optimal writing regimes for 213 nm laser light in a planar silica platform. This study is not only critical for UV writing of waveguides, but also for Bragg gratings in predefined waveguides and local phase trimming [18].

2. Methodology

Prior to experiments, doped silica samples were placed in a high-pressure hydrogen cell at 120 bar for five days to enhance photosensitivity. SSDUW was used to define both channel waveguides and Bragg gratings by dual-beam interferometry with a pulsed 213 nm laser. A schematic of the SSDUW setup is shown in Fig. 1. More details can be found in [6], however, it should be noted

that here we are defining waveguides and gratings using the 213 nm light. A detailed fabrication methodology is provided in the fabrication section of the supplementary document.

A fifth harmonic solid-state Nd:YVO₄ laser operating at a wavelength of 213 nm (Xiton Photonics, Impress 213) was used as the writing source. The laser beam was expanded prior to splitting (using a beam splitter) to produce beams of an interferometer. The resulting interference fringes were used to define the periodic refractive index modulation of the Bragg gratings. One beam of the interferometer is passed through a bespoke DKDP electro-optic modulator (EOM, Leysop Ltd), which provides phase control of the interference pattern. Both beams are focused to the same position by using a pair of CaF₂ planoconvex lenses. The precision air-bearing stage system is used to translate the sample underneath the beams. With the correct modulation of the EOM, a channel waveguide containing a Bragg grating is formed. The omission of modulation causes smearing of the induced refractive index change resulting in a channel waveguide without a grating [6]. The crossing angle of the two beams was maintained at 22.6° (half angle 11.3°), which corresponds to a fringe period of 535.6 nm and a Bragg wavelength within the silica of ~1550 nm. The sample to be written is translated through the focal spot using precision air-bearing stages (Aerotech ABL 9000). The EOM permits phase control of the gratings, allowing different periods to be written using demodulation. This process is referred to as 'grating detuning' [6,16]. For this experiment, the repetition rate of the laser was fixed at 12.5 kHz to generate a maximum average power of 30 mW (at the surface of chip).

In order to evaluate the effect of average power and fluence on grating properties, a chip of 20×10 mm was selected and UV written with a series of integrated waveguides and gratings. Each waveguide was 8.1 mm long and contained one 4 mm long uniform grating at a targeted Bragg wavelength of 1540 nm, followed by a 1.5 mm long grating at a Bragg wavelength of 1560 nm. In each waveguide, the 1540 nm grating served to estimate the coupling loss during characterization and was fabricated with 95% EOM duty cycle to make the grating highly saturated. The typical coupling loss to standard optical fiber is 0.6 dB. The details are available in the supplementary document. The second grating was shorter (1.5 mm) and fabricated with lower duty cycle (50%) in an effort to make strong but not highly saturated gratings as they provide a poor regime for

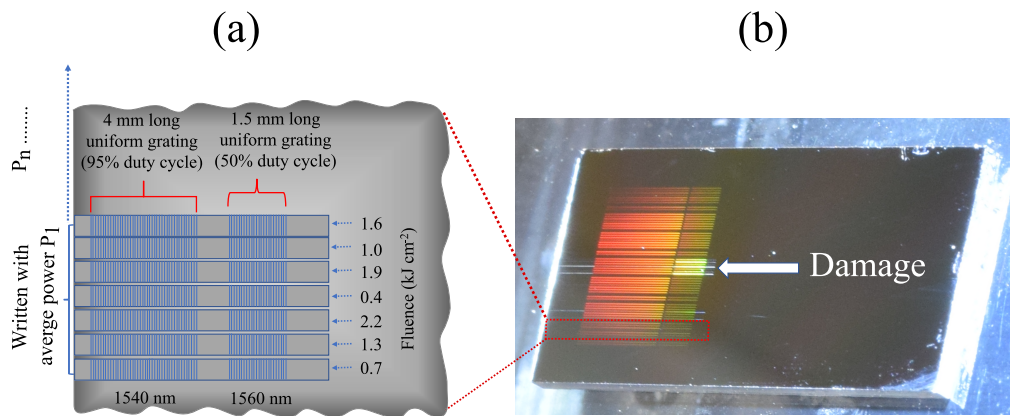


Fig. 2. (a) Schematic of a single set of gratings and waveguides written at a defined average power (P_1), showing the different fluences used in each set. The fluence was controlled by varying stage speed. (b) Photograph of the UV written chip mounted on the characterisation apparatus showing seven sets of waveguides written as different average powers. A white light source highlights the diffraction of the Bragg gratings. The waveguides written with higher average power (7.3 and 11.6 mW) show signs of laser-induced damage, observed as white lines.

interrogating the properties of the grating. For a fixed writing power, a set of seven waveguides was fabricated at fluences ranging from 0.4 to 2.2 kJ cm⁻² in a pseudo-random order. The fluence was controlled by the translation speed of the air-bearing stage system. The chip contained seven similar sets of waveguides fabricated at writing powers ranging from 0.6 to 11.6 mW corresponding to peak laser intensities of 0.02 to 0.58 GW cm⁻², as shown in Fig. 2(a). The writing power of the beam was controlled using ND filters. Increasing the average power while maintaining constant fluence results in an increase of the translation speed of the stage system; the sample is exposed to higher pulse energies but a smaller number of pulses. Additionally, the chip contained eight other test waveguides to monitor the alignment and effects of hydrogen out-gassing. We observed no obvious variation in the properties of the device due to out-gassing or alignment. The grating characterisation was performed in TE and TM using a polarized output of Er-doped fiber amplifier ASE source [17]. A 3 dB fused fiber coupler was used to collect the reflected light, and the grating spectra were measured on an optical spectrum analyzer. Figure 2(b) shows a photograph of the UV fabricated chip; the white light illumination shows the colorful diffraction of the Bragg gratings. The waveguides written with a higher average power of 7.3 and 11.6 mW showed signs of laser-induced damage. The origin of this damage formation is briefly discussed in the supplementary document (see Figure S2).

3. Results and analysis

The dependence of grating characteristics (bandwidth, reflection, etc) on laser writing power and fluence are non-trivial, so we explore them independently. Firstly, we investigate the effect of varying fluence at constant power, later we discuss the effect of varying writing power at a constant fluence.

Figure 3 displays the reflection spectra of the gratings from one of the alignment waveguides written at a fluence of 1 kJ cm⁻² and 3.6 mW average writing power. See Figure S3 to visualize data on a linear scale. The reflectivity of these gratings was normalized by reference to the 3.3% reflection of the ASE source from the pigtail facet. We used the Rouard's method [19] to model and fit the experimental spectra. This process returns the central wavelength of the peak and the gratings modulation depth Δn_{ac} . The effective refractive index of the mode (n_{eff}) is calculated from the central Bragg wavelength using the Bragg condition of the inscribed grating period.

Figure 4 shows a plot of variation in n_{eff} and Δn_{ac} for each 1.5 mm long grating as a function of writing fluence at different average powers. At all writing powers, the n_{eff} response shows a similar trend (as seen in [16]) where a positive increase in the effective refractive index is observed. The n_{eff} response associated with the red shift in central wavelength and can be explained typically on the basis of photo-chemical changes in color centers due to laser exposure. However, it is interesting to observe the different trends in grating modulation Δn_{ac} as a function of writing powers and fluence. At low powers of 0.6 and 1.8 mW, we observe an increase in Δn_{ac} followed by saturation with increasing fluence from 0.4 to 2.2 kJ cm⁻². On increasing the writing power from 2.6 to 7.3 mW, the Δn_{ac} increases to a peak value of 5.1×10^{-4} around a fluence of 1 kJ cm⁻², and begins to reduce with a further increase in fluence. In this power range, the response of Δn_{ac} can be well understood by looking at the response of the n_{eff} . At the lower fluences, the grating modulation increases with fluence, as does n_{eff} , as expected. However, at higher fluences, where the photosensitivity begins to saturate, the gratings reflectivity and Δn_{ac} reduces. This has previously been observed by others working with high fluence exposures [20], and is a consequence of both photosensitivity saturation and non-perfect visibility of the inscription system. At the highest power of 11.6 mW, we observe an entirely different response in grating strength. However, as we observe damage in these waveguides, it is difficult to trust the reflectivity measurements due to the perceived increase in loss. Figure S4 presents the same data as in Fig. 4, but as a function of power at the different fluences. We do not observe any negative change in refractive index as a function of laser fluence. Contrary to our observations, Pissadakis

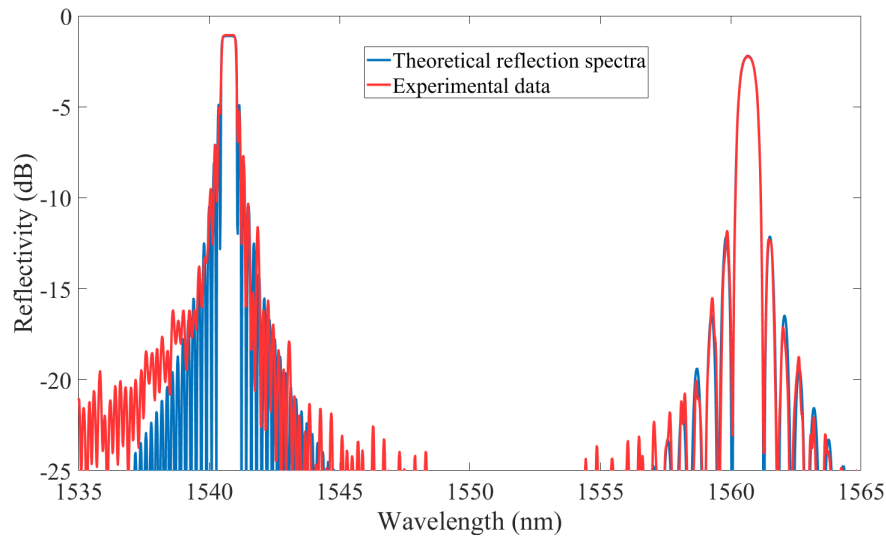


Fig. 3. Experimentally measured spectra of 4 mm and 1.5 mm long uniform gratings, fabricated at 3.6 mW writing power and the fluence of 1 kJ cm^{-2} are plotted on a dB scale. In this plot, experimental data is shown in red, and the theoretical reflection spectra of an ideal uniform Bragg reflector are plotted in blue. See the supplementary document for modelling details.

[21] have reported the transition of gratings from type I to type II in B/Ge doped hydrogen-free fibers in a similar fluence range of 1 to 3 kJ cm^{-2} ; although in their work a picosecond laser was used. Furthermore, it is difficult to compare our grating properties to FBG due to different compositions of doped silica, hydrogen-loaded samples, and fabrication methods.

Figure 4 provided a comparison between the change in the n_{eff} and Δn_{ac} . To demonstrate the dependence of n_{eff} on writing power and fluence, we plot n_{eff} as a function of fluence (on a linear-log scale) in Fig. 5. A similar plot of n_{eff} as a function of laser pulses per micron is shown in Figure S5 of the supplementary document and provides an alternative route to visualize the data in Fig. 5. At all writing powers we observe that n_{eff} increases logarithmically and follows a linear trend line on linear-log scale. At lower writing powers ranging from 0.6 to 4.6 mW, the gradient of linear trend lines agrees within error. However, the differing offset (increased n_{eff}) within a fluence range of 0.4 to 2.2 kJ cm^{-2} shows that the photosensitivity of the B/Ge doped silica does not only depend upon fluence, as previously discussed, but also on the average power (i.e. intensity of exposure). Increasing the writing power to 7.3 and 11.6 mW leads to a lower gradient compared to what we observe with lower average powers, as shown in Fig. 5. This shows that the photosensitivity response is dependent on the average writing power (in the instance when cumulative exposure is equal), specifically higher average powers leads to greater photosensitivity, but also results in saturation (roll-off) occurring at lower fluences. We would expect to have the same value of n_{eff} at zero fluence suggesting a nonlinear trend between fluence zero and 0.4 kJ cm^{-2} . However, it is challenging to evaluate the photosensitivity response of a planar sample at very low fluences due to the absence of a pre-defined channel waveguide.

We also observed variation in the birefringence ($n_{\text{eff}}^{\text{TM}} - n_{\text{eff}}^{\text{TE}}$) depending upon writing power and fluences shown in Fig. 6. The inherent birefringence appears to be 1×10^{-4} due to stress and geometry of our planar silica-on-silicon structure. At the lowest writing power of 0.6 mW, increasing writing fluence does not lead to significant variation. With an increasing writing power, birefringence follows a negative correlation with the fluence as was seen previously with

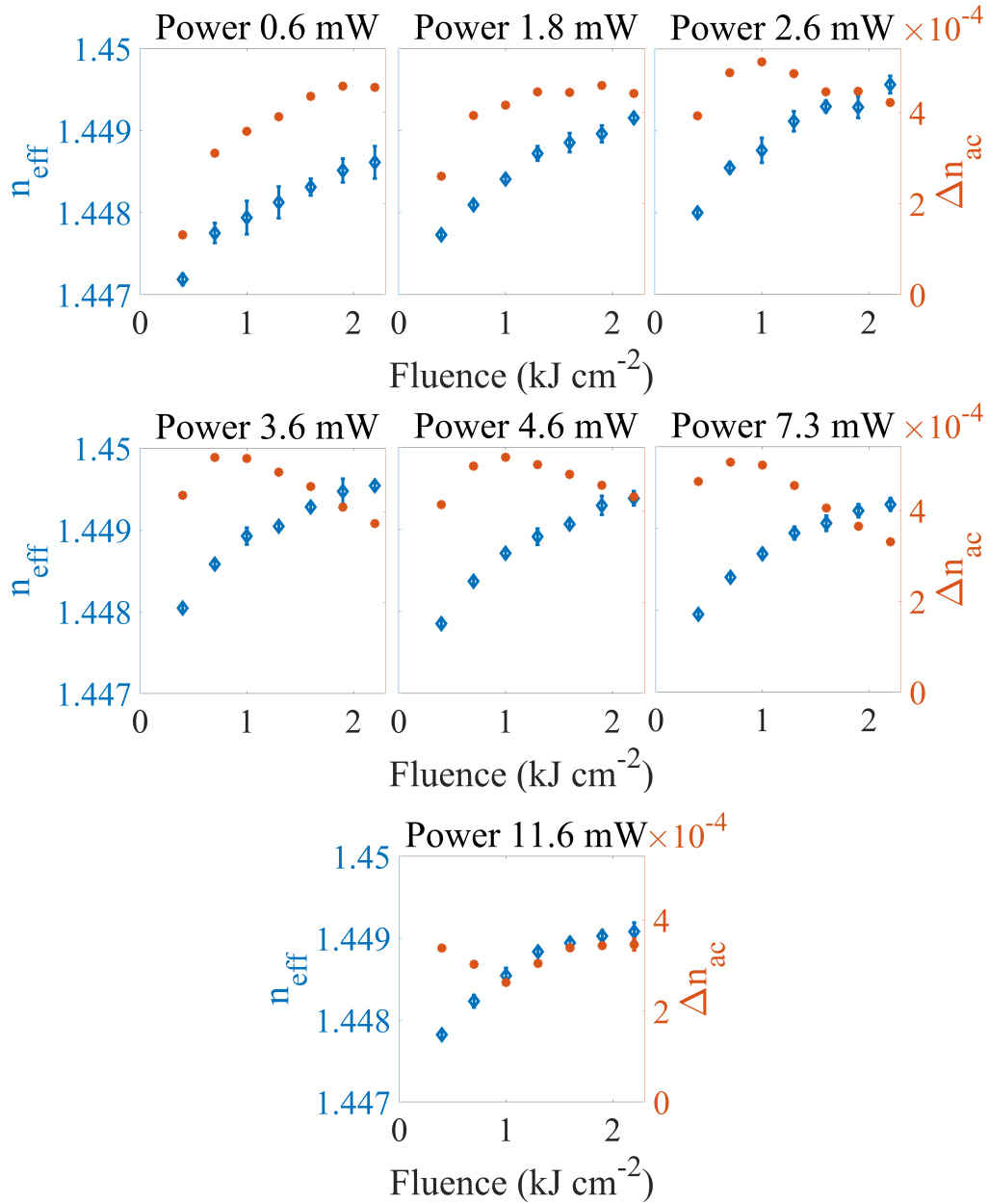


Fig. 4. Plot of n_{eff} and Δn_{ac} as a function of fluence at writing beam powers ranging from 0.6 to 11.6 mW.

244 nm laser processing [22]. UV writing increases the refractive index of the core layer, which can reduce the birefringence due to modal power confinement. Additionally, local stresses near the waveguide can also dominate stress-induced polarization effects. Figures 5 and 6 clearly demonstrate that the writing power in 213 nm laser inscription is a crucial parameter to decide the response of photosensitivity. Devices made with the lowest writing power of 0.6 mW show the lowest n_{eff} for all fluences; correspondingly these waveguides written at 0.6 mW are the most birefringent.

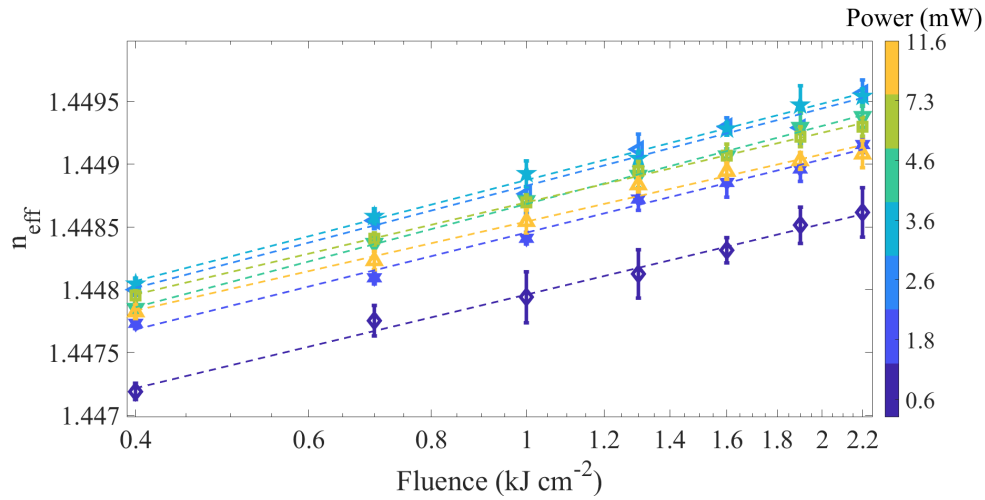


Fig. 5. Plot of n_{eff} as a function of fluence in a linear-log scale.

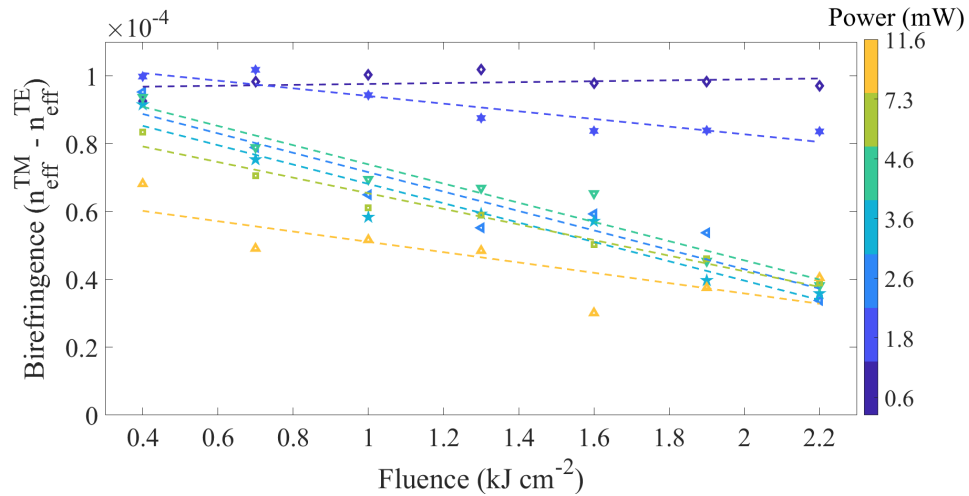


Fig. 6. Birefringence measurement as a function of increasing fluence at writing powers ranging from 0.6 to 11.6 mW.

UV writing experiments using a CW 244 nm laser is conventionally expected to exhibit a photosensitivity response proportional to fluence, and independent of the writing power. However, the variation in photosensitivity and birefringence with increasing writing power (using a pulsed 213 nm laser) may be associated to the pulsed nature of laser and thermal effects. Additionally, it is also possible that higher pulse energies no longer follow the same photosensitivity model as the lower and more than one physical process, such as heating and damage is involved in determining the net change in refractive index [20]. The different photosensitivity behaviours in this experiment could potentially be described by a mixing of the photo-induced chemical changes and densification-related process. The photo-induced chemical mechanism gives a positive refractive index change, saturating when all species have been reacted, whereas densification can lead to more complex refractive index behaviour. It is possible that at higher powers the Kramers-Kronig effect is being dominated by a densification or damage-related process.

4. Conclusion

For the first time, we have extensively investigated the regimes (power and fluence relationship) of SSDUW using 213 nm light. This paper discusses the non-typical effects of writing power and fluence on the induced effective change in the refractive index and gratings strength. Compared to [11,23], we have used higher peak intensities (up to 0.58 GW cm^{-2}) to define waveguides and Bragg gratings in doped silica. Contrary to [11], we have not seen any significant evidence of similar non-linear photosensitivity response in B/Ge silica. However, we do observe a subtle non-linearity where gratings and waveguide properties depend on writing power. However, it is challenging to draw comparisons due to the different compositions of glass, the geometry of planar sample and effect of doping and hydrogen loading. We observe that writing powers of 2.5 to 4.6 mW are ideal for SSDUW, where we suppose the change in the refractive index upon laser exposure is dominated by photochemical changes. In this writing regime, grating strength is maximum at a fluence of 1 kJ cm^{-2} and the photosensitivity response appears to be optimum, an essential feature to fabricate complex devices. The maximum value of Δn_{ac} observed in this study is 5.1×10^{-4} . However, the grating strength is intentionally reduced for these experiments and we can achieve Δn_{ac} up to 1.25×10^{-3} which is higher compared to 244 nm writing experiments [6]. Above powers of 4.6 mW, the data suggests additional refractive index change caused by damage-induced stress and leads to photosensitivity saturation at lower fluences and reduced grating strength. Light microscopy also showed that the use of high writing power leads to localized damage of the silica-silicon interface. This work enables direct UV writing with 213 nm laser light, as a route to local phase trimming of dielectric materials.

Funding. Innovate UK (50414); Engineering and Physical Sciences Research Council (EP/M013243/1, EP/M013294/1, EP/M024539/1, EP/T00097X/1, EP/T001062/1, EP/V053213/1); Royal Academy of Engineering Senior Research Fellowship (RCSRF1718639).

Acknowledgment. The authors would like to acknowledge Xiton Photonics GMBH for outstanding support and excellent service.

Disclosures. The authors declare no conflicts of interest.

Data availability. All data supporting this study are openly available from the University of Southampton repository in [24].

Supplemental document. See Supplement 1 for supporting content.

References

1. M. Y. Park, W. Yoon, S. Han, and G. H. Song, "Fabrication of low-cost planar wavelength-selective optical add-drop multiplexer by employing UV photosensitivity," *Electron. Lett.* **38**(24), 1532–1533 (2002).
2. N. M. Davis, S. G. Lynch, J. C. Gates, J. Hodgkinson, P. G. R. Smith, and R. P. Tatam, "Spectroscopic gas detection using a Bragg grating-stabilized external cavity laser, custom written in planar integrated silica-on-silicon," *Opt. Express* **27**(20), 29034–29044 (2019).
3. C. Holmes, J. C. Gates, L. G. Carpenter, H. L. Rogers, R. M. Parker, P. A. Cooper, S. Chaotan, F. R. M. Adikan, C. B. E. Gawith, and P. G. R. Smith, "Direct UV-written planar Bragg grating sensors," *Meas. Sci. Technol.* **26**(11), 112001 (2015).
4. X. C. Luo, C. Chen, L. Qin, X. Zhang, Y.-y. Chen, B. Wang, L. Liang, P. Jia, Y. Q. Ning, and L. J. Wang, "High-birefringence waveguide Bragg gratings fabricated in a silica-on-silicon platform with displacement Talbot lithography," *Opt. Mater. Express* **10**(10), 2406–2414 (2020).
5. G. Douglass, F. Dreisow, S. Gross, S. Nolte, and M. J. Withford, "Towards femtosecond laser written arrayed waveguide gratings," *Opt. Express* **23**(16), 21392–21402 (2015).
6. C. Sima, J. C. Gates, H. L. Rogers, P. L. Mennea, C. Holmes, M. N. Zervas, and P. G. R. Smith, "Ultra-wide detuning planar Bragg grating fabrication technique based on direct UV grating writing with electro-optic phase modulation," *Opt. Express* **21**(13), 15747–15754 (2013).
7. J. Canning, "Fibre gratings and devices for sensors and lasers," *Laser Photonics Rev.* **2**(4), 275–289 (2008).
8. L. Skuja, "Optically active oxygen-deficiency-related centers in amorphous silicon dioxide," *J. Non. Cryst. Solids* **239**(1-3), 16–48 (1998).
9. D. Hand and P. S. J. Russell, "Photoinduced refractive-index changes in germanosilicate fibers," *Opt. Lett.* **15**(2), 102–104 (1990).
10. A. Gusarov and D. Doyle, "Contribution of photoinduced densification to refractive-index modulation in Bragg gratings written in Ge-doped silica fibers," *Opt. Lett.* **25**(12), 872–874 (2000).

11. M. Gagné and R. Kashyap, "New nanosecond Q-switched Nd:VO₄ laser fifth harmonic for fast hydrogen-free fiber Bragg gratings fabrication," *Opt. Commun.* **283**(24), 5028–5032 (2010).
12. P. C. Gow, R. H. S. Bannerman, P. L. Mennea, C. Holmes, J. C. Gates, and P. G. R. Smith, "Direct UV written integrated planar waveguides using a 213 nm laser," *Opt. Express* **27**(20), 29133–29138 (2019).
13. R. Kashyap, *Fiber Bragg Gratings* (Academic Press, 2009).
14. P. C. Gow, Q. S. Ahmed, P. L. Mennea, R. H. S. Bannerman, A. Jantzen, C. Holmes, J. C. Gates, C. B. E. Gawith, and P. G. R. Smith, "213 nm laser written waveguides in Ge-doped planar silica without hydrogen loading," *Opt. Express* **28**(21), 32165–32172 (2020).
15. Q. S. Ahmed, P. C. Gow, P. L. Mennea, R. H. S. Bannerman, D. H. Smith, C. Holmes, J. C. Gates, and P. G. R. Smith, "Direct 213 nm UV written Bragg gratings and waveguides in planar silica without hydrogen loading," in *Integrated Photonics Research, Silicon and Nanophotonics*, (Optical Society of America, 2020), pp. IW2A–4.
16. Q. S. Ahmed, P. C. Gow, C. Holmes, P. L. Mennea, J. W. Field, R. H. Bannerman, D. H. Smith, C. B. E. Gawith, P. G. Smith, and J. C. Gates, "Direct UV written waveguides and Bragg gratings in doped planar silica using a 213 nm laser," *Electron. Lett.* **57**(8), 331–333 (2021).
17. P. C. Gow, Q. S. Ahmed, J. C. Gates, P. G. R. Smith, and C. Holmes, "Microwave consolidation of UV photosensitive doped silica for integrated photonics," *Opt. Mater. Express* **11**(6), 1835–1841 (2021).
18. H. L. Rogers, S. Ambran, C. Holmes, P. G. R. Smith, and J. C. Gates, "In situ loss measurement of direct UV-written waveguides using integrated Bragg gratings," *Opt. Lett.* **35**(17), 2849–2851 (2010).
19. A. S. Othonos and K. Kalli, *Fiber Bragg Gratings Fundamentals and Applications in Telecommunications and Sensing* (Artech House, 1999).
20. K. P. Chen, P. R. Herman, R. Taylor, and C. Hnatovsky, "Vacuum-ultraviolet laser-induced refractive-index change and birefringence in standard optical fibers," *J. Lightwave Technol.* **21**(9), 1969–1977 (2003).
21. S. Pissadakis and M. Konstantaki, "Type IIA gratings recorded in B-Ge codoped optical fibre using 213 nm Nd:YAG radiation," in *2005 31st European Conference on Optical Communication, ECOC 2005*, vol. 3 (IET, 2005), pp. 563–564.
22. C. Holmes, P. A. Cooper, H. N. Fernando, A. Stroll, J. C. Gates, C. Krishnan, R. Haynes, P. L. Mennea, L. G. Carpenter, C. B. E. Gawith, M. M. Roth, M. D. Charlton, and P. G. R. Smith, "Direct UV written planar Bragg gratings that feature zero fluence induced birefringence," *Meas. Sci. Technol.* **26**(12), 125006 (2015).
23. S. Pissadakis and M. Konstantaki, "Grating inscription in optical fibres using 213 nm picosecond radiation: a new route in silicate glass photosensitivity," in *Proceedings of 2005 7th International Conference Transparent Optical Networks, 2005.*, vol. 1 (IEEE, 2005), pp. 337–342.
24. Q. S. Ahmed, J. W. Field, C. Holmes, S. Z. Oo, P. L. Mennea, J. W. Field, R. H. S. Bannerman, R. Cecil, G. Churchill, C. B. E. Gawith, P. G. R. Smith, P. C. Gow, and J. C. Gates, "Dataset for investigation into the writing dynamics of planar Bragg gratings using pulsed 213 nm radiation," Soton, 2022, <https://doi.org/10.5258/SOTON/D2179>.